Saharan and Arabian dust Forcing: IR and solar data from TERRA and TRMM

V. Ramanathan, F. Li and A. Inamdar

Center for Clouds, Chemistry and Climate,
Scripps Institution of Oceanography,
University of California, San Diego

MOTIVE

DUST: Ranking No. 1 in the aerosol family

Estimates of present-day global emission of major aerosol types (in Tg/yr)

Source	Low	High	Best
Natural			
Soil dust (mineral aerosol)	1,000	3,000	1,500
Sea-salt	1,000	10,000	1,300
Volcanic dust	4	10,000	33
Biological debris	26	80	50
Sulphates	64	155	102
Organics from biogenic NMHC[a]	40	200	55
Nitrates from NO_x	10	40	22
Anthropogenic			
Industrial dust	40	130	100
Black carbon (soot and charcoal)	10	30	20
Sulphates	120	180	140
Biomass burning	50	140	80
Nitrates from NO_x	20	50	36
Organics from anthropogenic NMHC[a]	5	25	10
Total	2,390	24,000	3,450

[a]NMHC, non-methane hydrocarbons

Fig.1 Solar zenith match test with the original data (a) and after screening process (b).

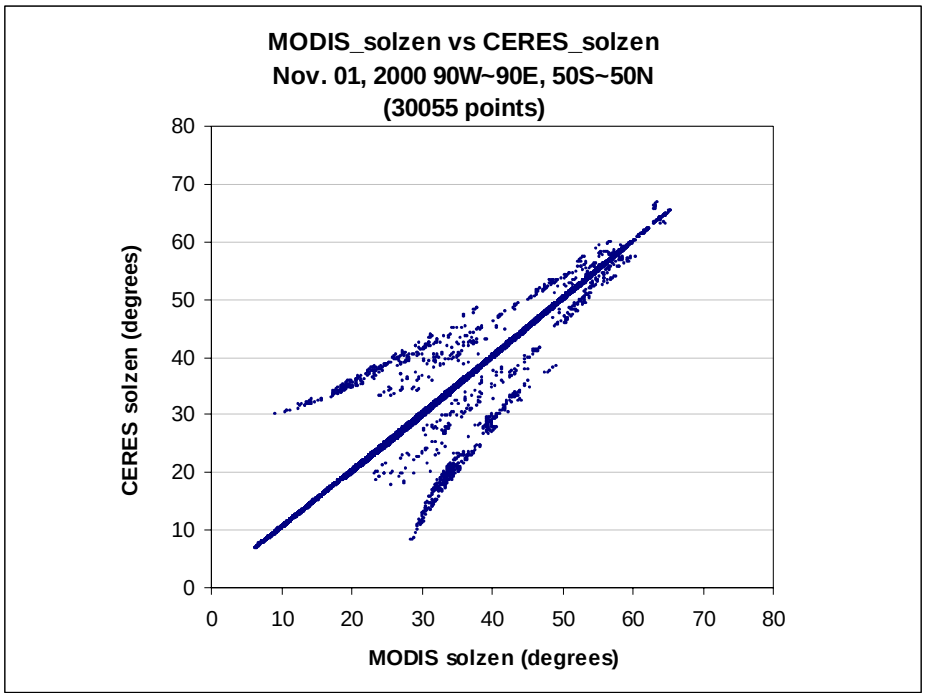

(a)

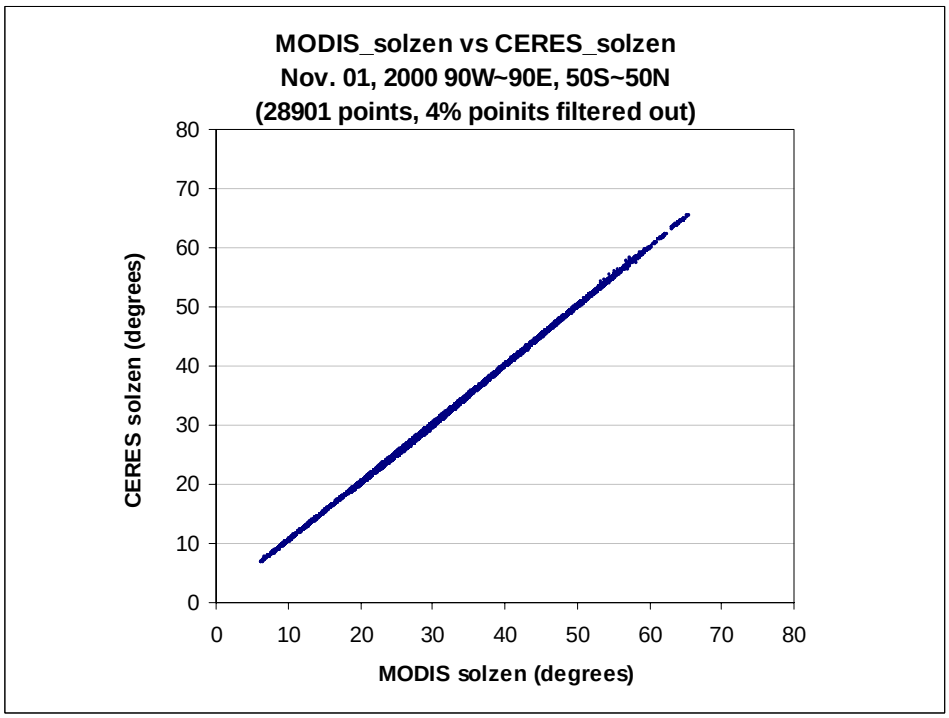

(b)

Fig. 2 MODIS dust aerosol plumes in Jul 2001 (a) and in Dec 2000(b)

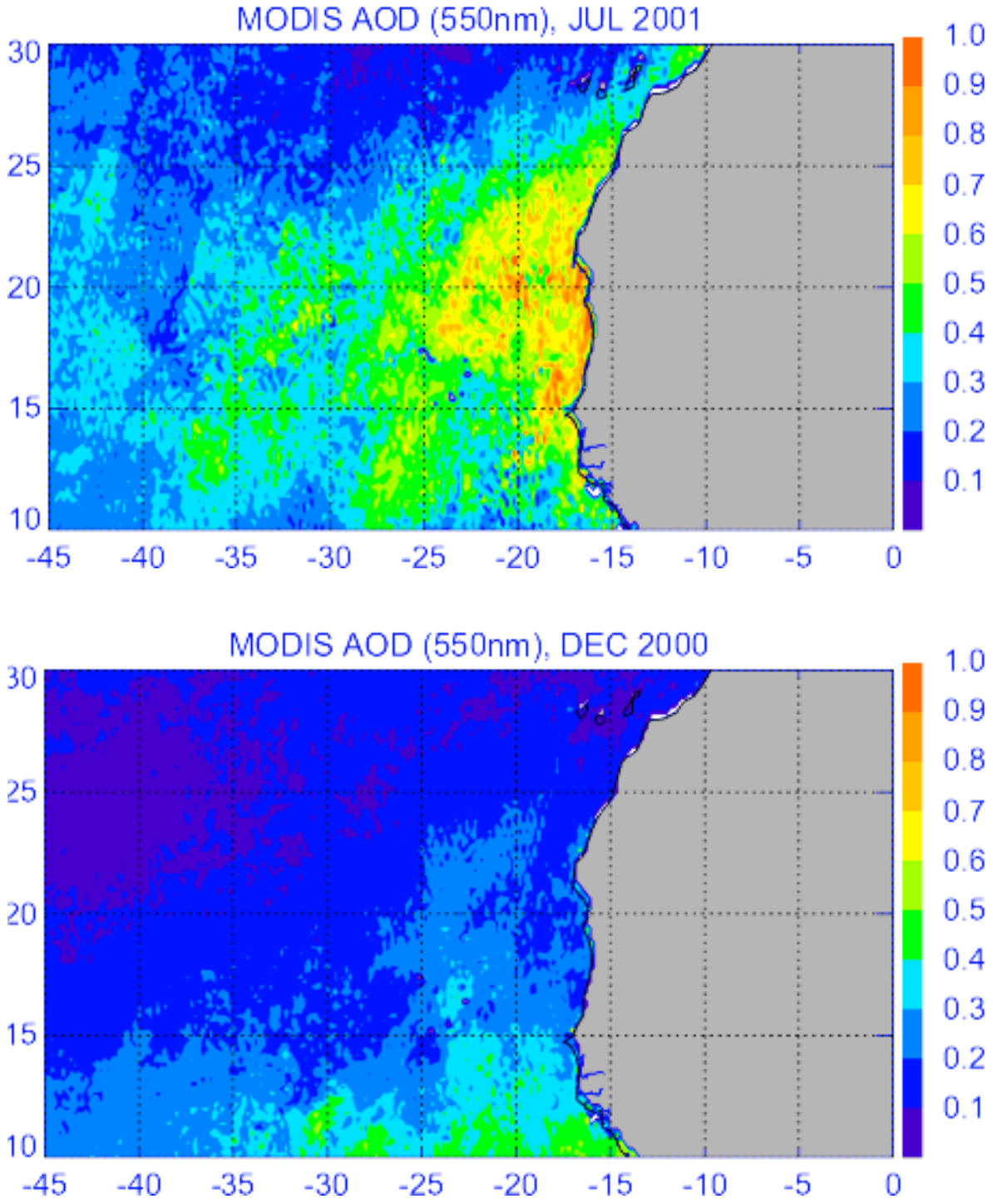

Fig.3 NCEP wind field distribution at 700mb layer in summer months (a) (Jun, Jul., and Aug.), and in winter months (b), (Nov, Dec., and Jan).

(

(

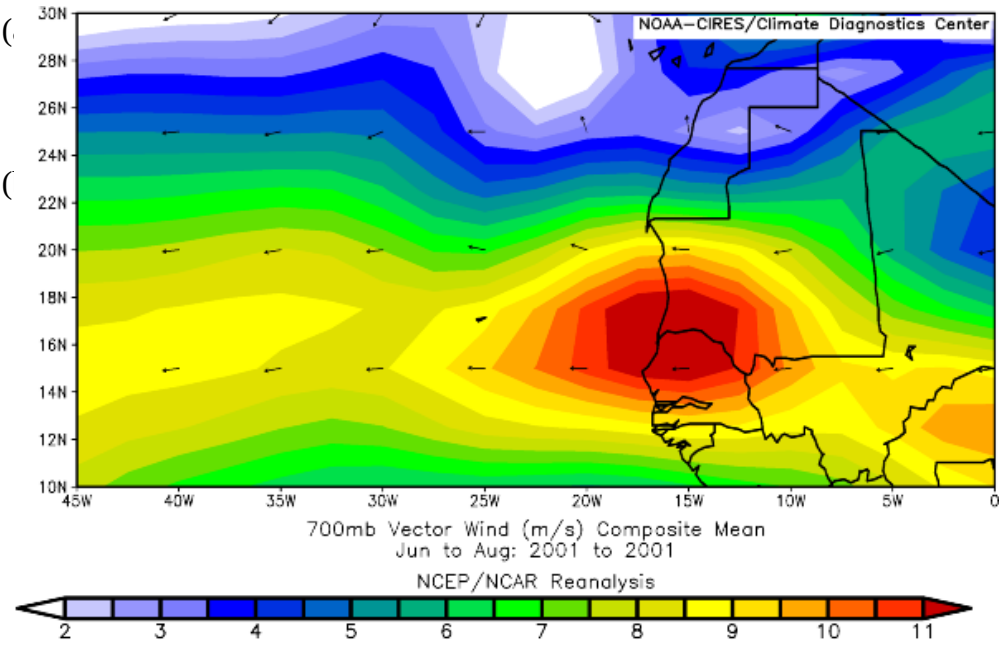

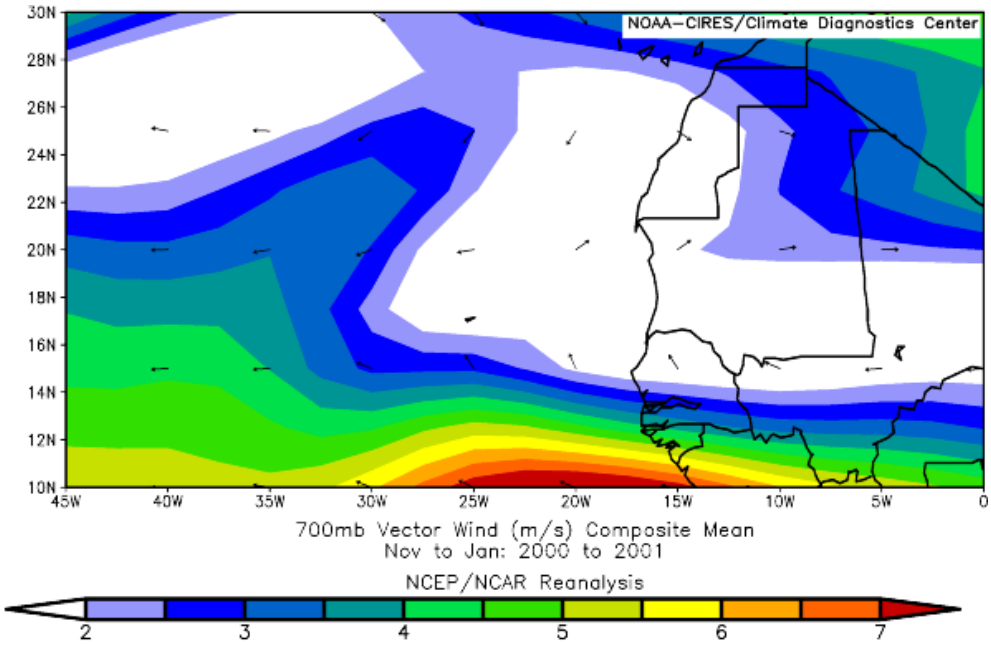

Fig. 4. MODIS monthly mean AOD (550nm) in the region of the northwest Africa (45W-0, 15N-25N).

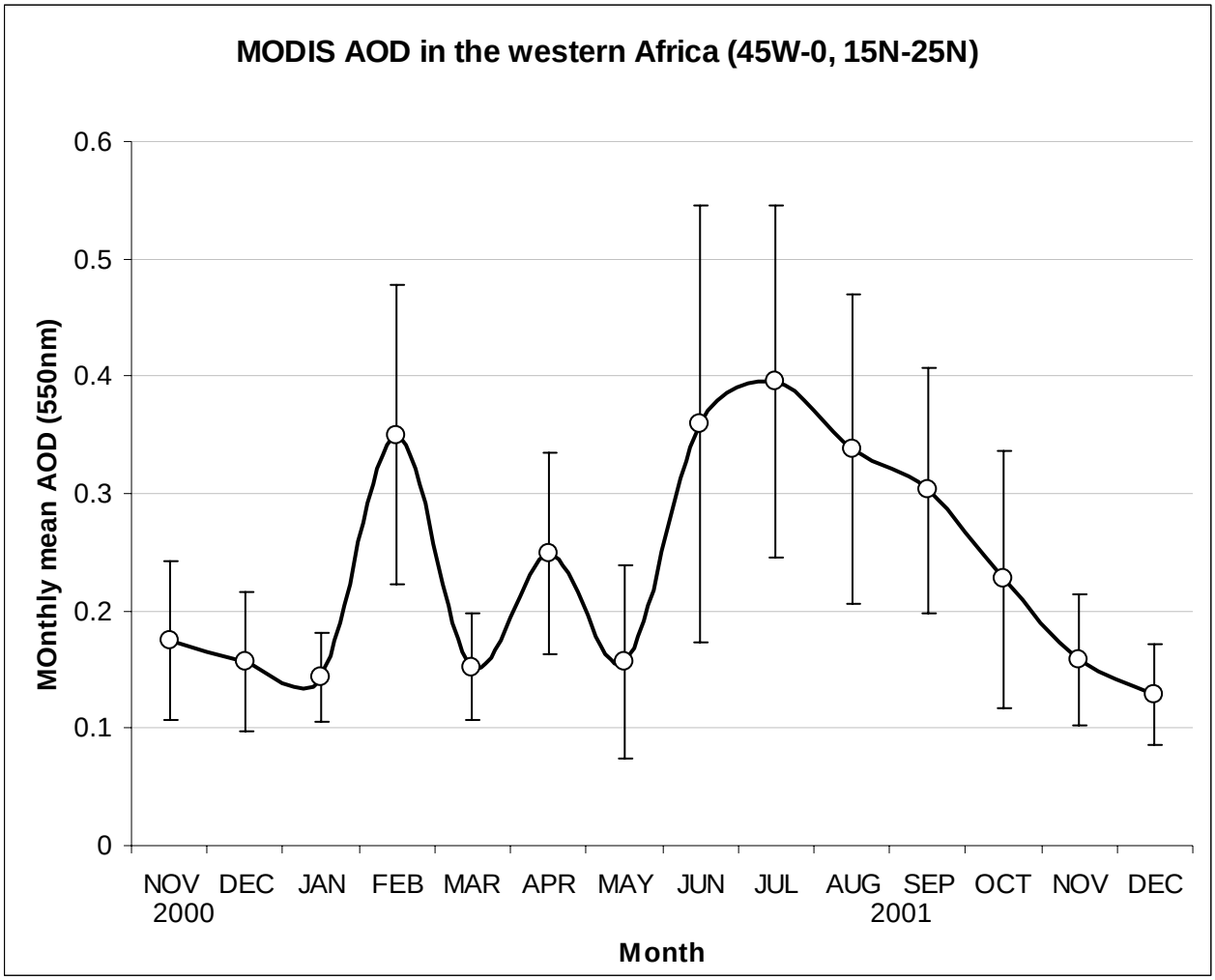

Fig. 5 Illustration of spring biomass burning aerosol invasion upon the dust targeted area with MODIS AOD distribution (a) and NCEP wind flow (b) in Feb. 2001

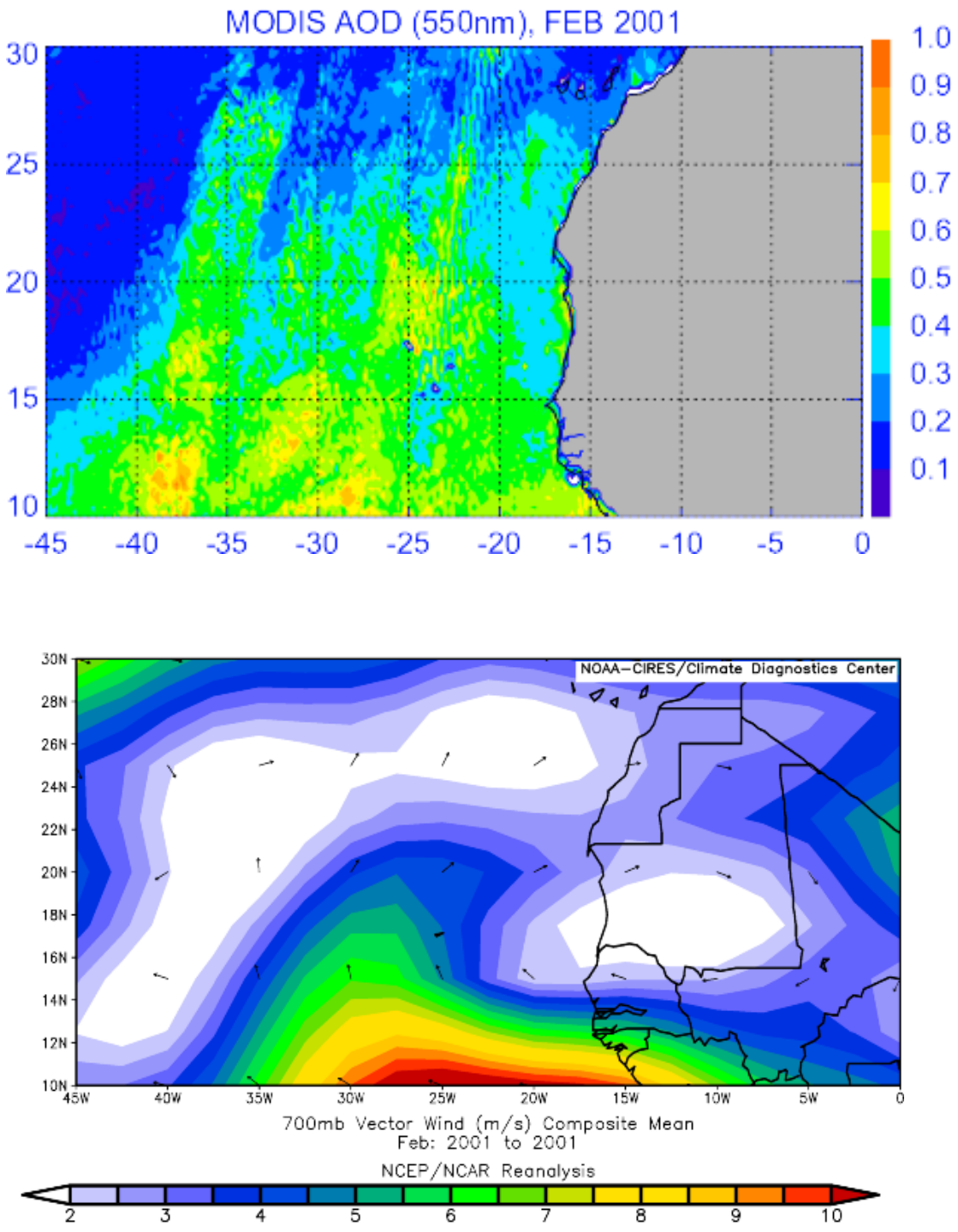

Fig. 6 MODIS dust aerosol effective radius in winter (Nov., Dec., and Jan), and in summer (Jun., Jul., and Aug.)

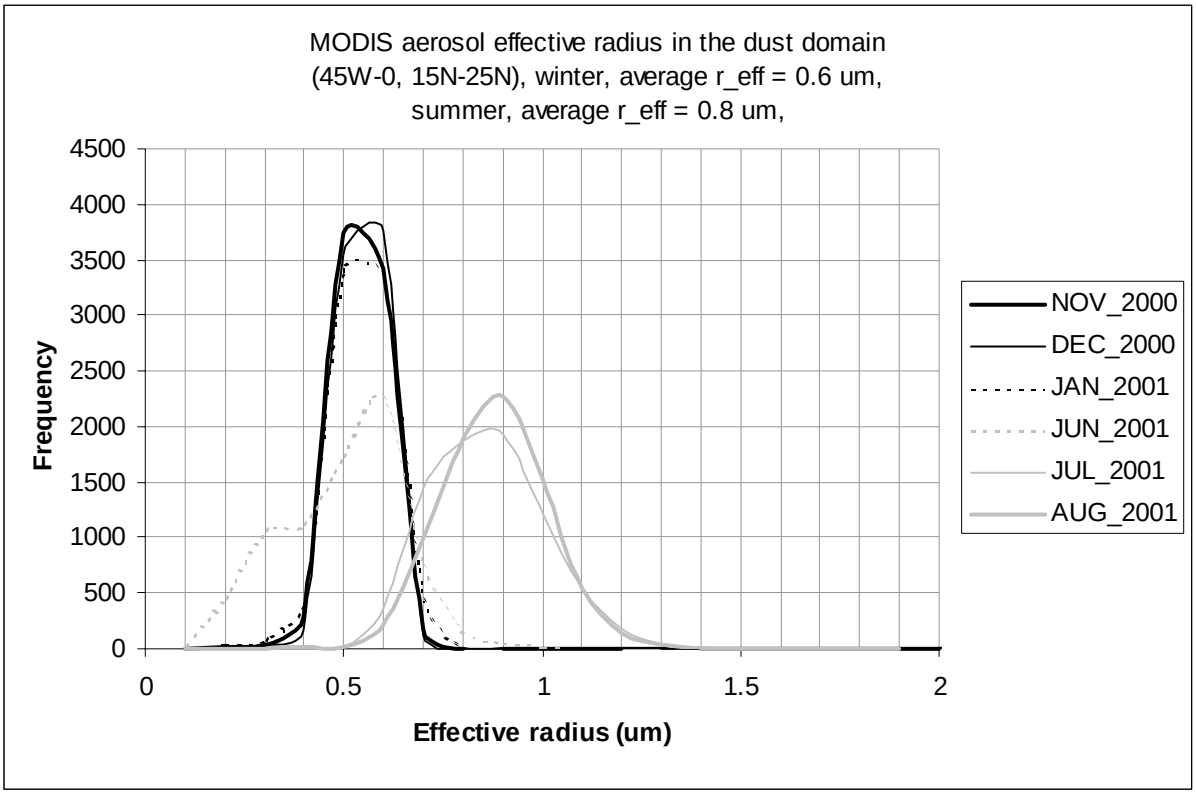

Fig. 7 Scatterplot of the CERES clear-sky TOA albedo and the corresponding collocated MODIS AOD over ocean off the northwest Africa in July, 2001(a), and in November 2000 (b).

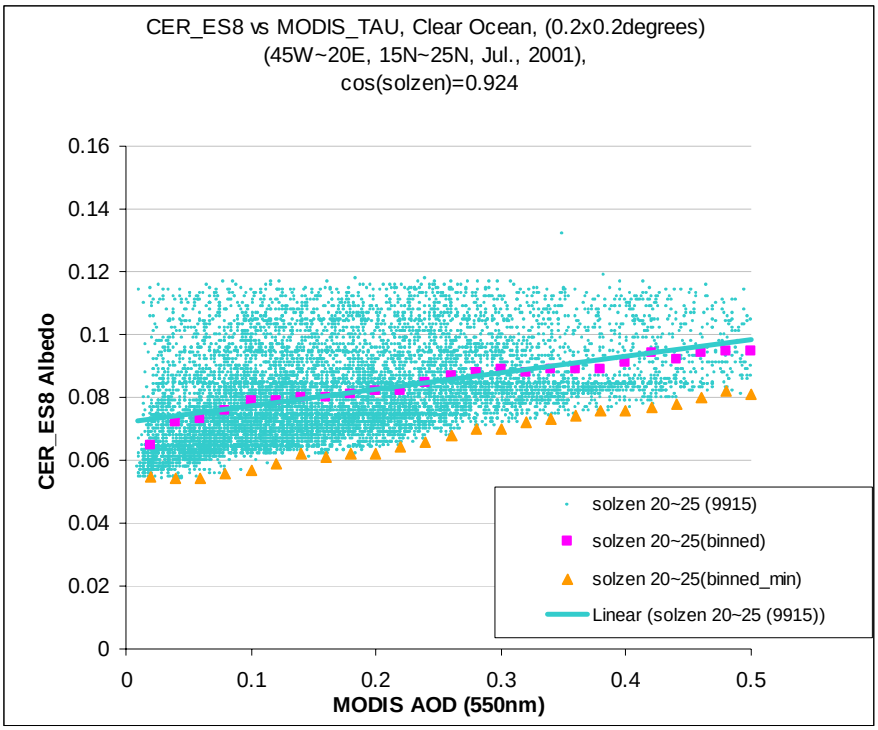

(a)

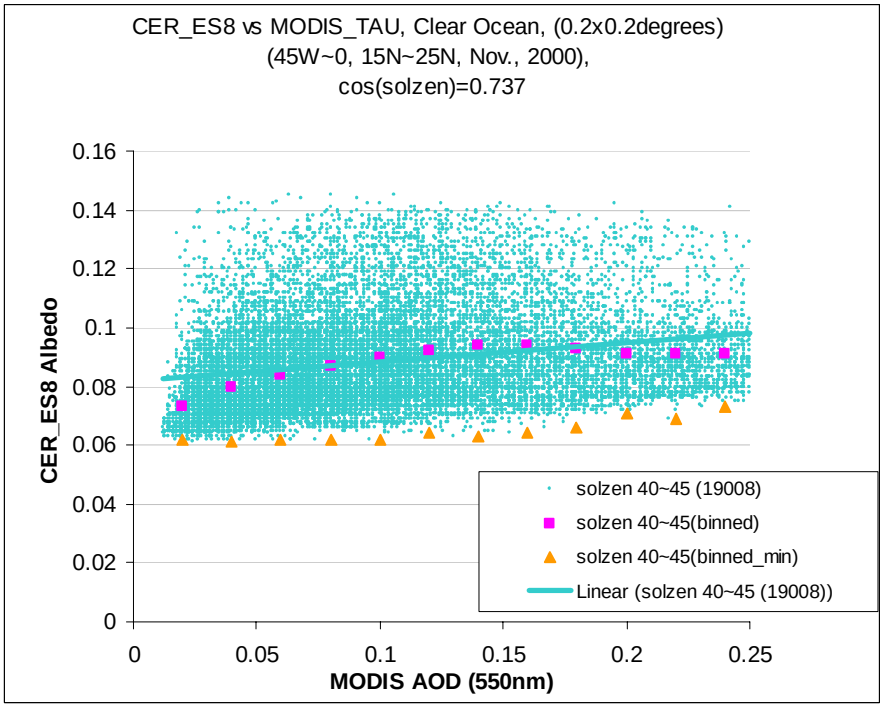

(b)

Fig. 8. Variation of the measured clear-sky dust aerosol radiative forcing efficiency (symbols) with the cosine solar zenith. in winter (a) and in summer (b). The solid lines shows the simulated dust aerosol forcing efficiency with the MODIS effective radius in figure 6.

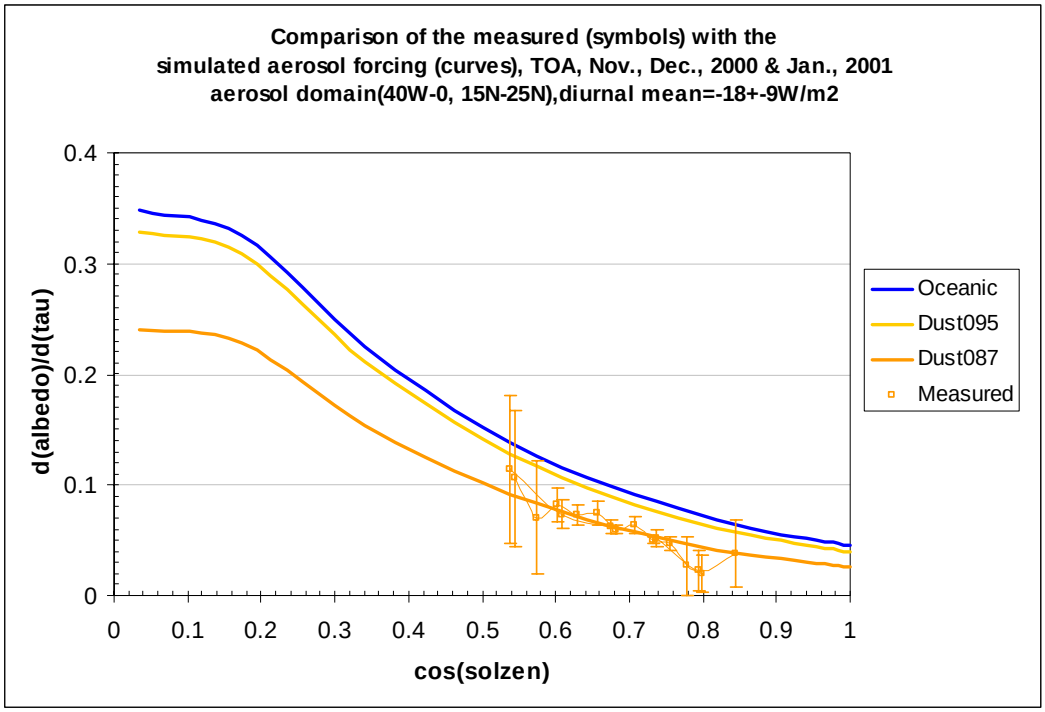

(a)

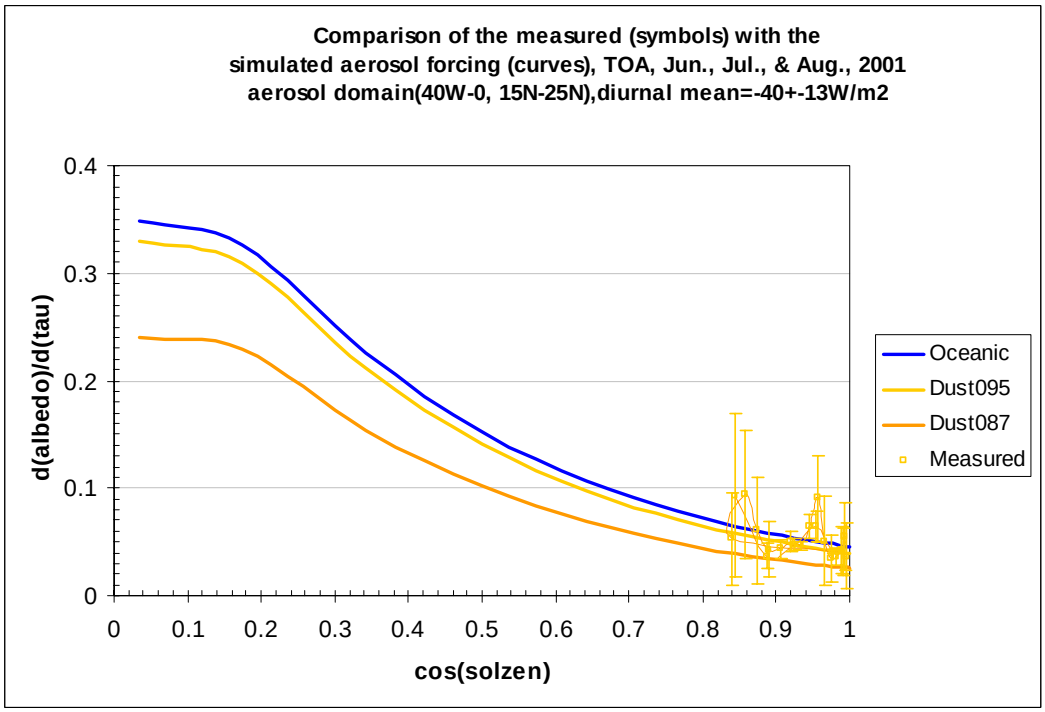

(b)

Fig. 9 Comparison of the dust single scattering albedo and asymmetry factor with the literature values.

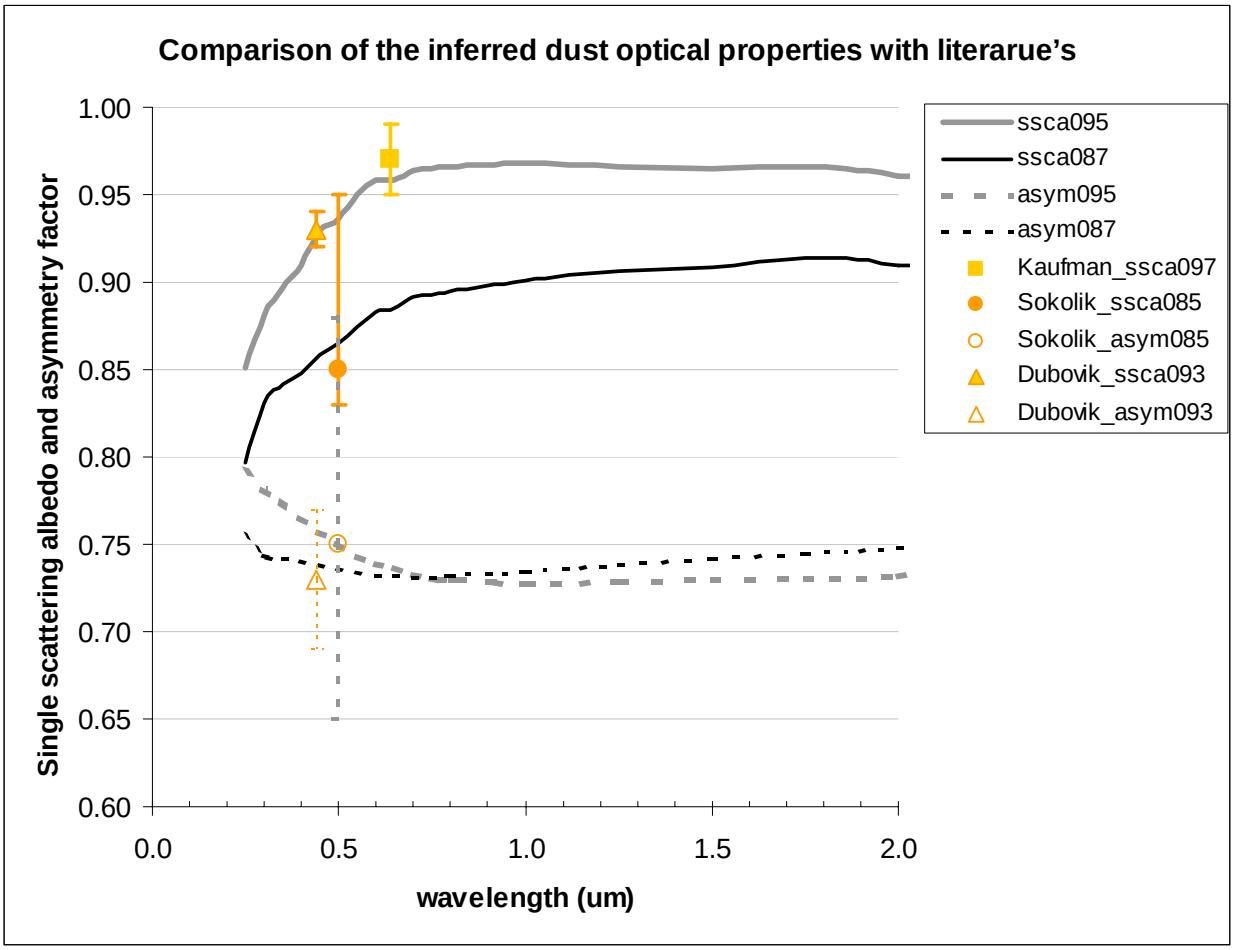

Fig. 10. MODIS scattering angel distribution on Nov 15, 2000 (a), and on Jul 15, 2001, and its histogram (c). Prepared for discussing dust non-spherical influence when Θ>120.

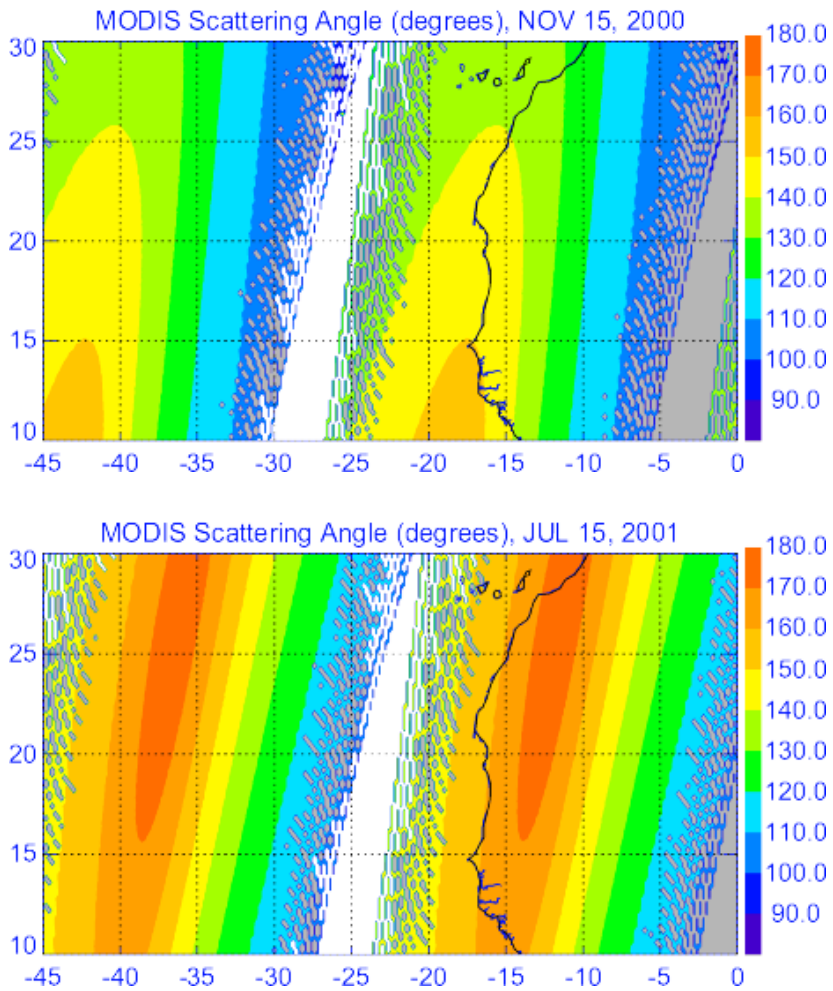

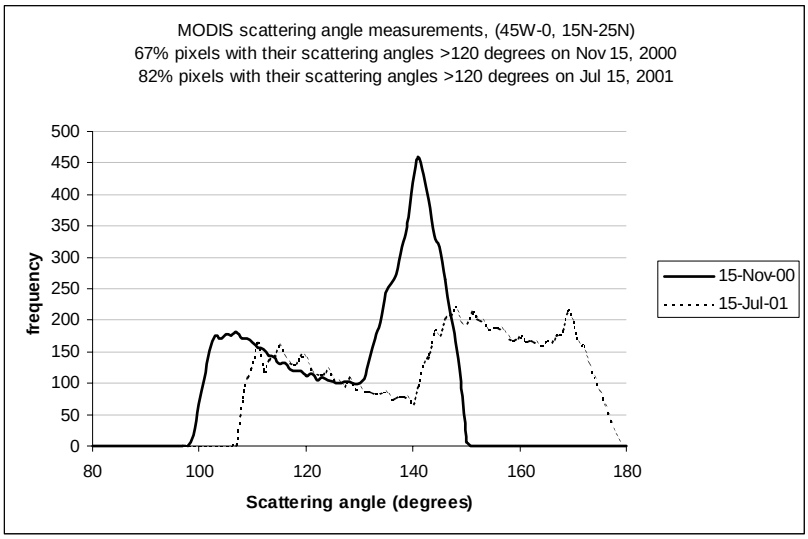

Table 1. Comparison of the dust forcing slopes from three linear-fitting methods, direct-fitting, binned-mean fitting, binned-minimum fitting.

Time	Solar zenith (degrees)	d(albedo)/dτ_a		
		direct-fitting	binned-mean	binned-min
Nov. 2000	35 ~ 40	0.049	0.045	0.050
	40 ~ 45	0.065	0.058	0.049
	45 ~ 50	0.068	0.055	0.052
Jul. 2001	15 ~ 20	0.050	0.042	0.047
	20 ~ 25	0.053	0.041	0.061
	25 ~ 30	0.058	0.046	0.050

Table 2. Comparison of dust aerosol radiative forcing with literatures.

No.	**ω_0**	**TOA** (Wm^{-2})	**Refs**
	0.87 ~ 0.95	**-18 ± 6 in winter** **-40 ± 11 in summer**	**our research MODIS, CERES**
1		**-60 ~ -81 (,** $\partial F / \partial AOT_{440}$ **July)**	**Weaver et al., J. Atmos. Sci., 59:736-747, 2002. TOMS, GCM, ERBE, Saharan Dust**
2	**0.92**	**-12.8 (over land, per AOD)** **-55.2 (over ocean)**	**Andreae et al., JGR, 107(D2)101029~, 2002 Nephelometer. Negev desert dust, Israel**
3	**0.87**	**-60 ± 5 (Apr. ,& May 1999)**	**James, et al, JGR, 106(D16),18417-,2001 Saharan dust , C-130**

Conclusions

1. **Diurnal mean dust forcing over ocean near the western Africa falls into –18 ± 6 W/m^2 in winter, and -40± 11 W/m^2 in summer.**

2. **The dust aerosol single scattering albedo undergoes variation from ~ 0.87 in winter to ~ 0.95 in summer.**

Winter to Summer Monsoon Variation of Aerosol Optical Depth Over the Tropical Indian Ocean

F. Li and V. Ramanathan
Center for Clouds, Chemistry and Climate,
Scripps Institution of Oceanography,
University of California, San Diego

(Journal of Geophysical Research, 170, 2002)

Plate 1

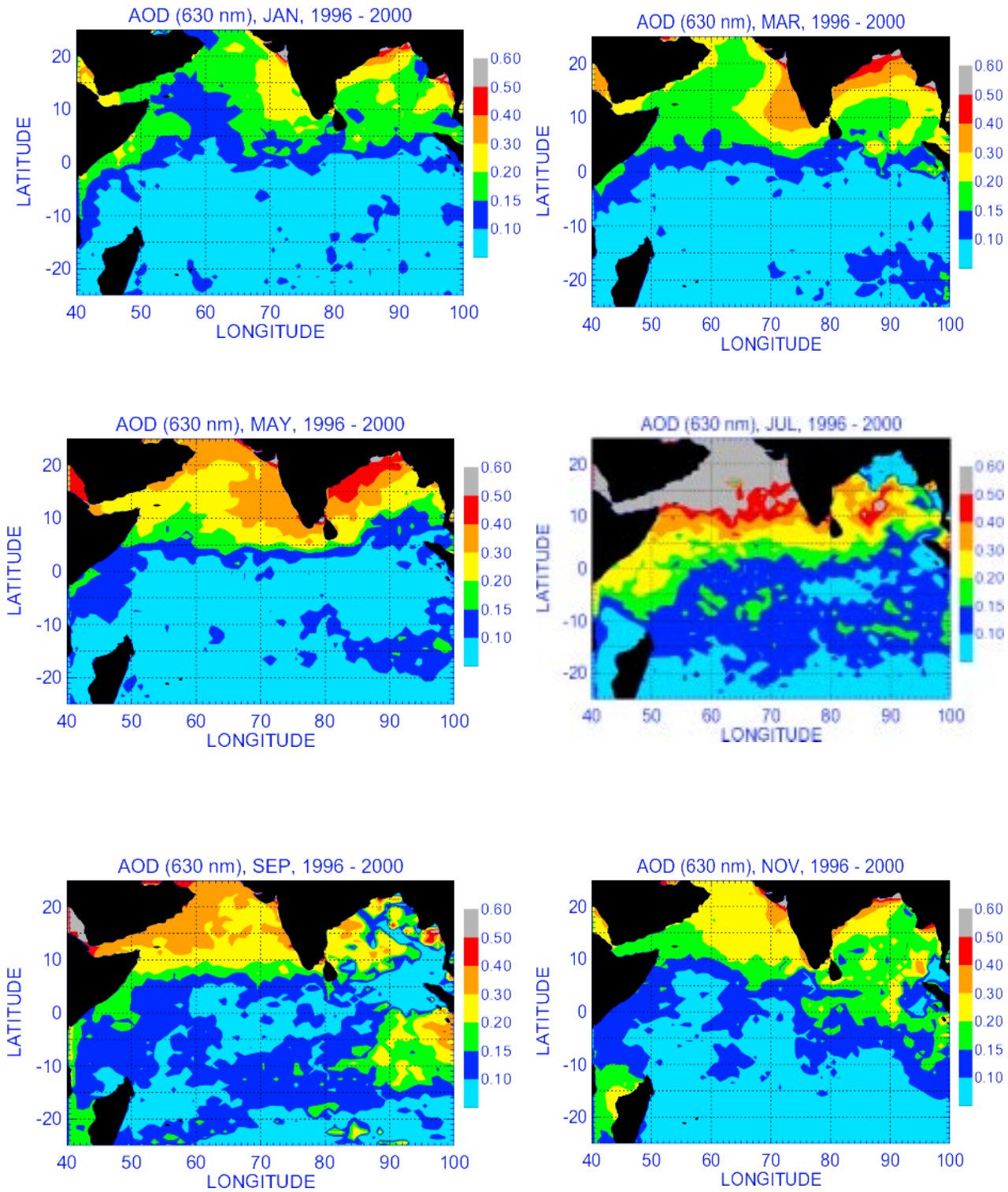
AOD (630 nm), JAN, 1996 - 2000
AOD (630 nm), MAR, 1996 - 2000
AOD (630 nm), MAY, 1996 - 2000
AOD (630 nm), JUL, 1996 - 2000
AOD (630 nm), SEP, 1996 - 2000
AOD (630 nm), NOV, 1996 - 2000
LATITUDE
LONGITUDE
20
10
0
-10
-20
40
50
60
70
80
90
100
0.60
0.50
0.40
0.30
0.20
0.15
0.10

Fig. 2

(a)

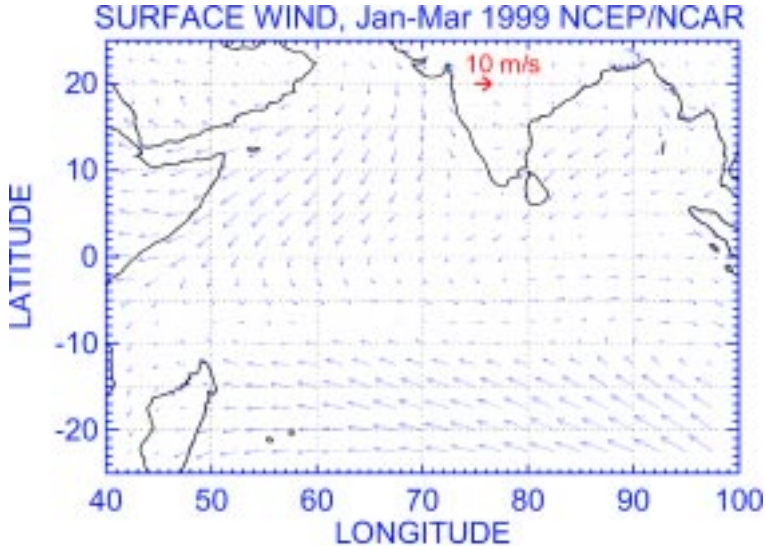
SURFACE WIND, Jan-Mar 1999 NCEP/NCAR
10 m/s
LATITUDE
20
10
0
-10
-20
40
50
60
70
80
90
100
LONGITUDE

(b)

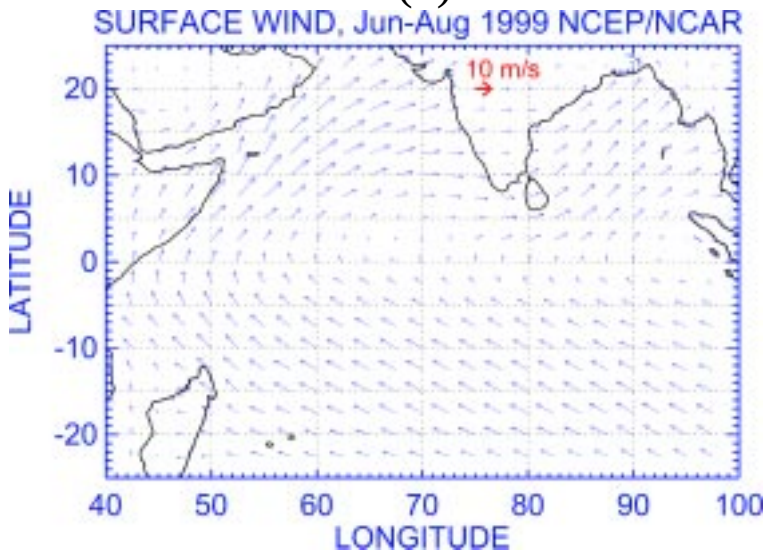
SURFACE WIND, Jun-Aug 1999 NCEP/NCAR
10 m/s
LATITUDE
20
10
0
-10
-20
40
50
60
70
80
90
100
LONGITUDE

(c)

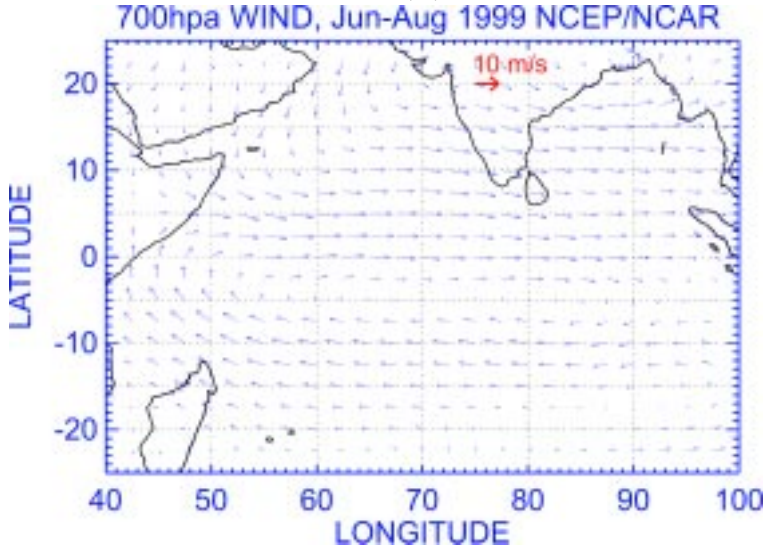
700hpa WIND, Jun-Aug 1999 NCEP/NCAR
10 m/s
LATITUDE
20
10
0
-10
-20
40
50
60
70
80
90
100
LONGITUDE

Fig4.

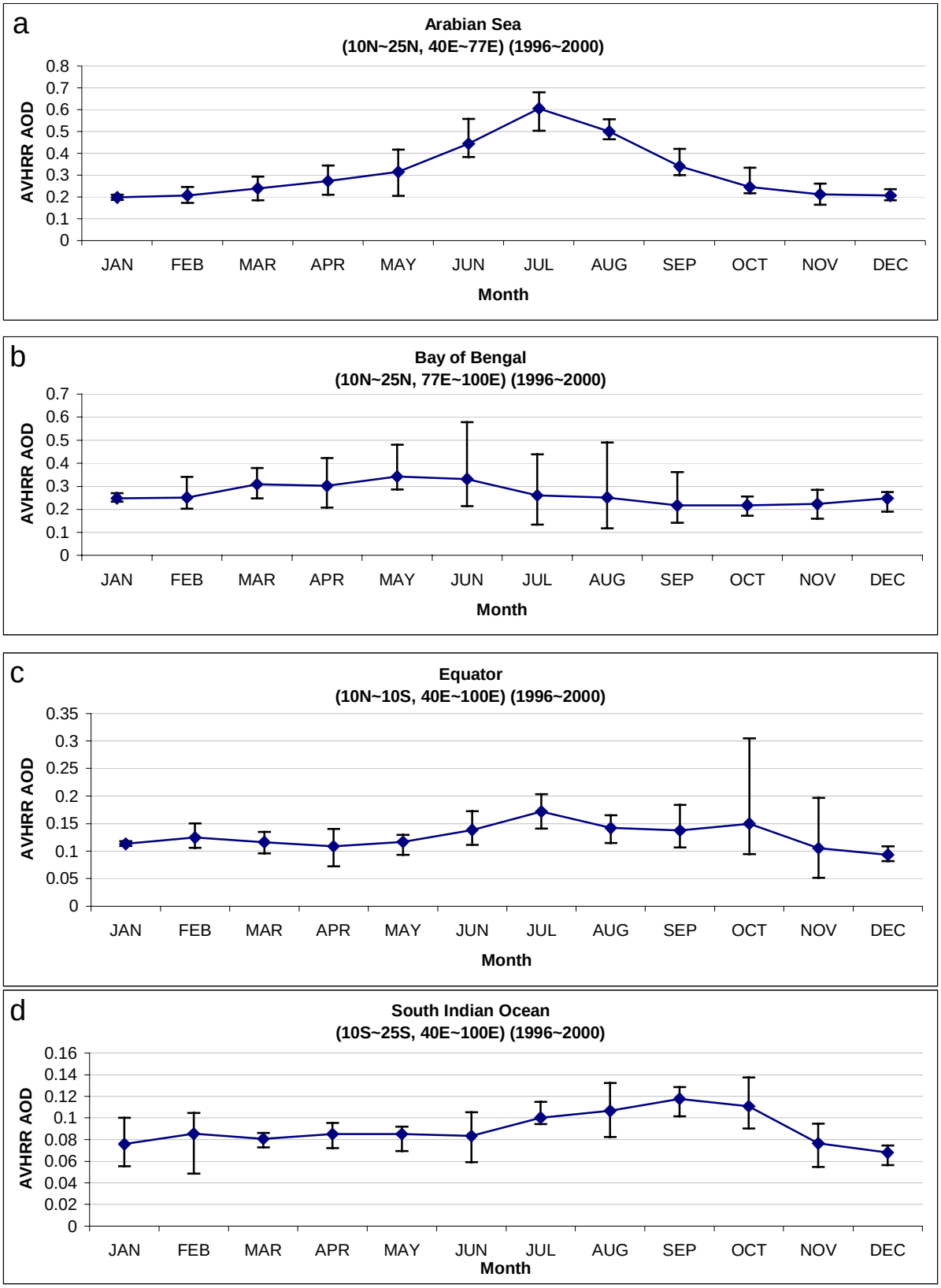
a
Arabian Sea
(10N~25N, 40E~77E) (1996~2000)
AVHRR AOD
0.8
0.7
0.6
0.5
0.4
0.3
0.2
0.1
0
JAN FEB MAR APR MAY JUN JUL AUG SEP OCT NOV DEC
Month
b
Bay of Bengal
(10N~25N, 77E~100E) (1996~2000)
AVHRR AOD
0.7
0.6
0.5
0.4
0.3
0.2
0.1
0
JAN FEB MAR APR MAY JUN JUL AUG SEP OCT NOV DEC
Month
c
Equator
(10N~10S, 40E~100E) (1996~2000)
AVHRR AOD
0.35
0.3
0.25
0.2
0.15
0.1
0.05
0
JAN FEB MAR APR MAY JUN JUL AUG SEP OCT NOV DEC
Month
d
South Indian Ocean
(10S~25S, 40E~100E) (1996~2000)
AVHRR AOD
0.16
0.14
0.12
0.1
0.08
0.06
0.04
0.02
0
JAN FEB MAR APR MAY JUN JUL AUG SEP OCT NOV DEC
Month

Radiative Forcing due to Mineral Dust Aerosol in the IR
V. Ramanathan and A. Inamdar

Domain: Arabian Sea (60 – 80 E, 10 – 30 N)

- Mineral dust aerosols play key role in climate forcing. Large uncertanties.

Even the sign of net forcing uncertain

- because of their non-spherical shape, model estimates are not reliable.

- ***MODIS on TERRA with CERES gives us the first opportunity***

to obtain the forcing directly from observations; and thus provide an independent data set to understand the importance of non-spherical shapes and unknown dust chemical composition.

We have just begun looking at the dust in Arabian sea; Next we will look at Saharan dust

AVHRR-DERIVED AOD (630 nm) MATCHED WITH CERES FOOTPRINTS: JJA 1998

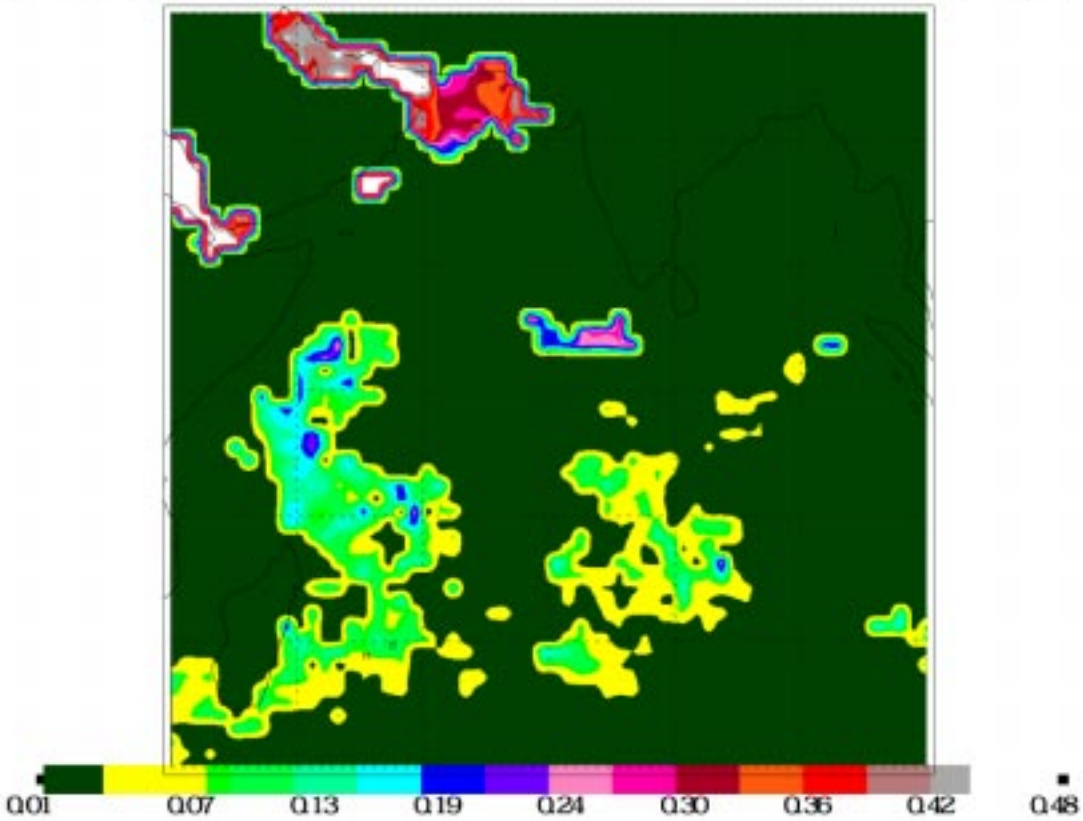

Window flux is influenced by in addition to AOD, total moisture loading in the atmosphereic column and temperature.

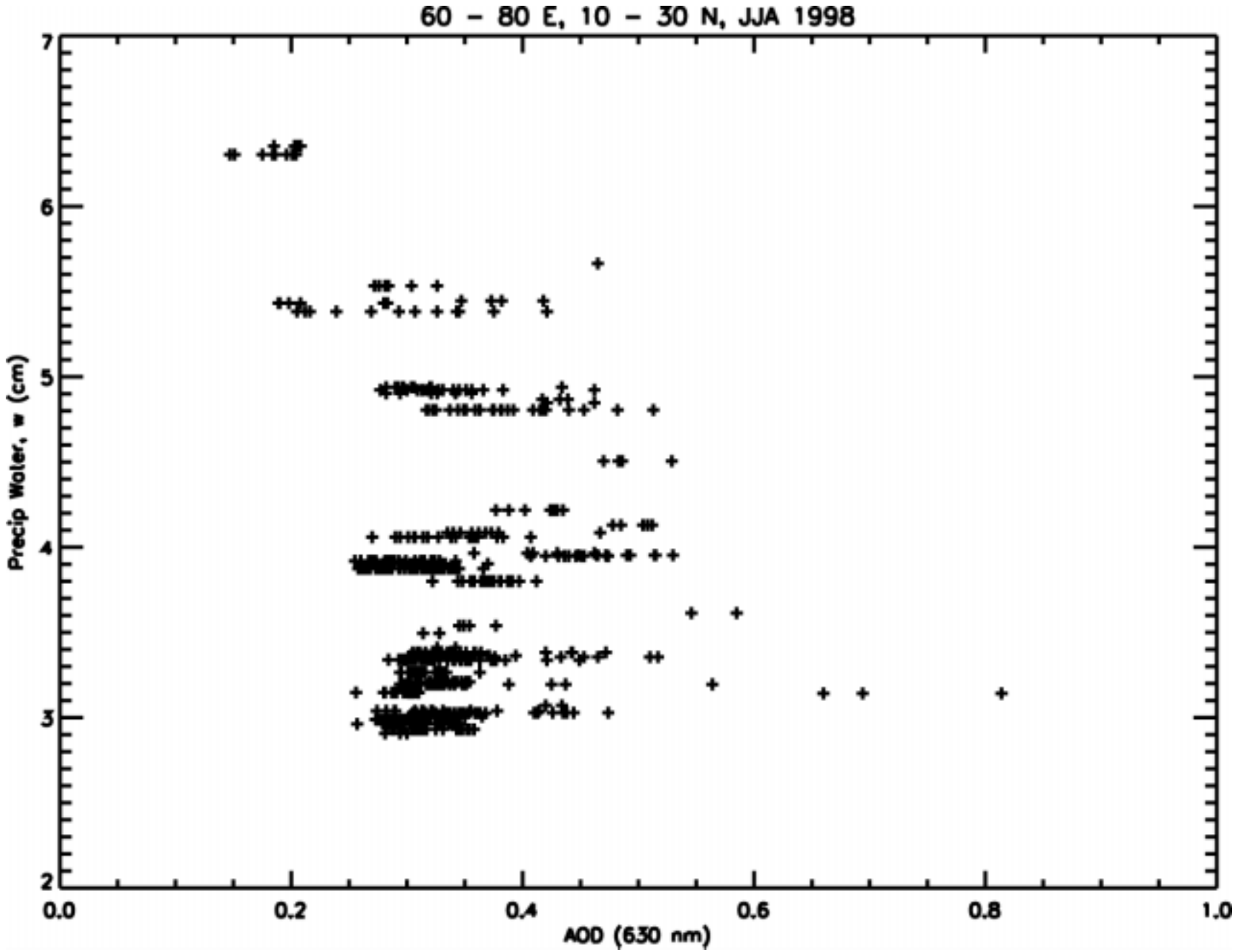
60 – 80 E, 10 – 30 N, JJA 1998
Precip Water, w (cm)
AOD (630 nm)
0.0
0.2
0.4
0.6
0.8
1.0
2
3
4
5
6
7

PRECIP WATER (cm): JJA 1998

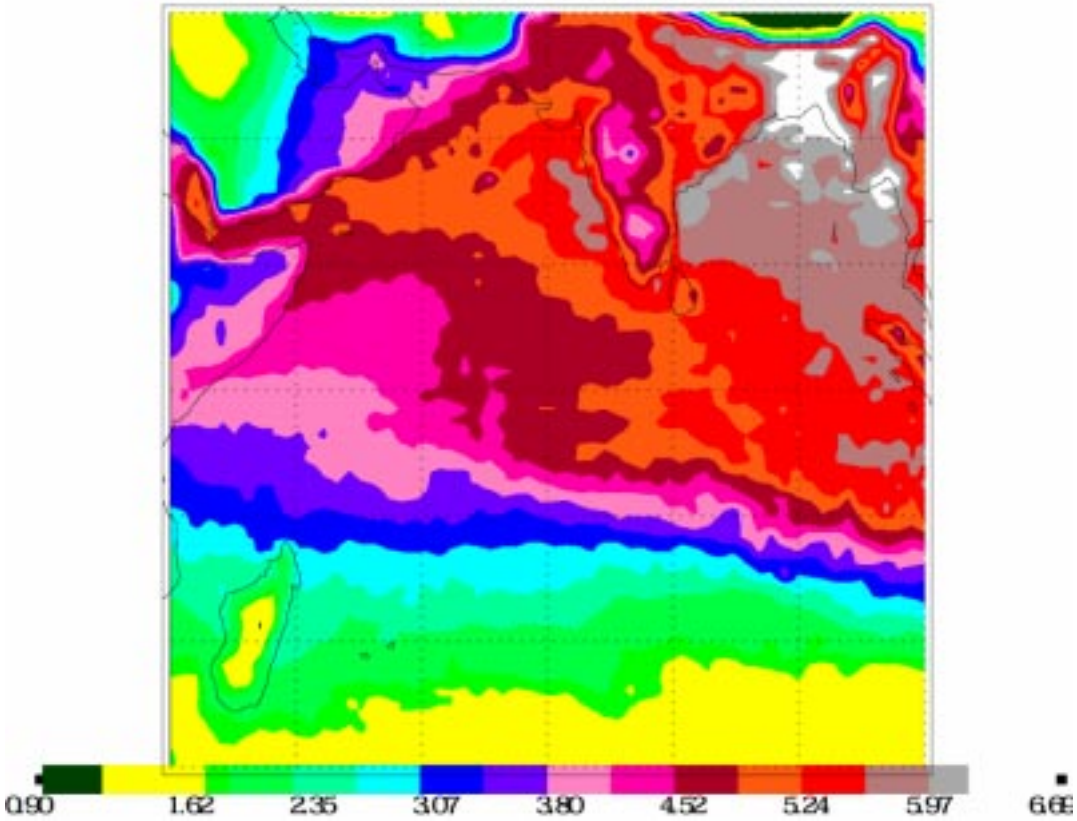

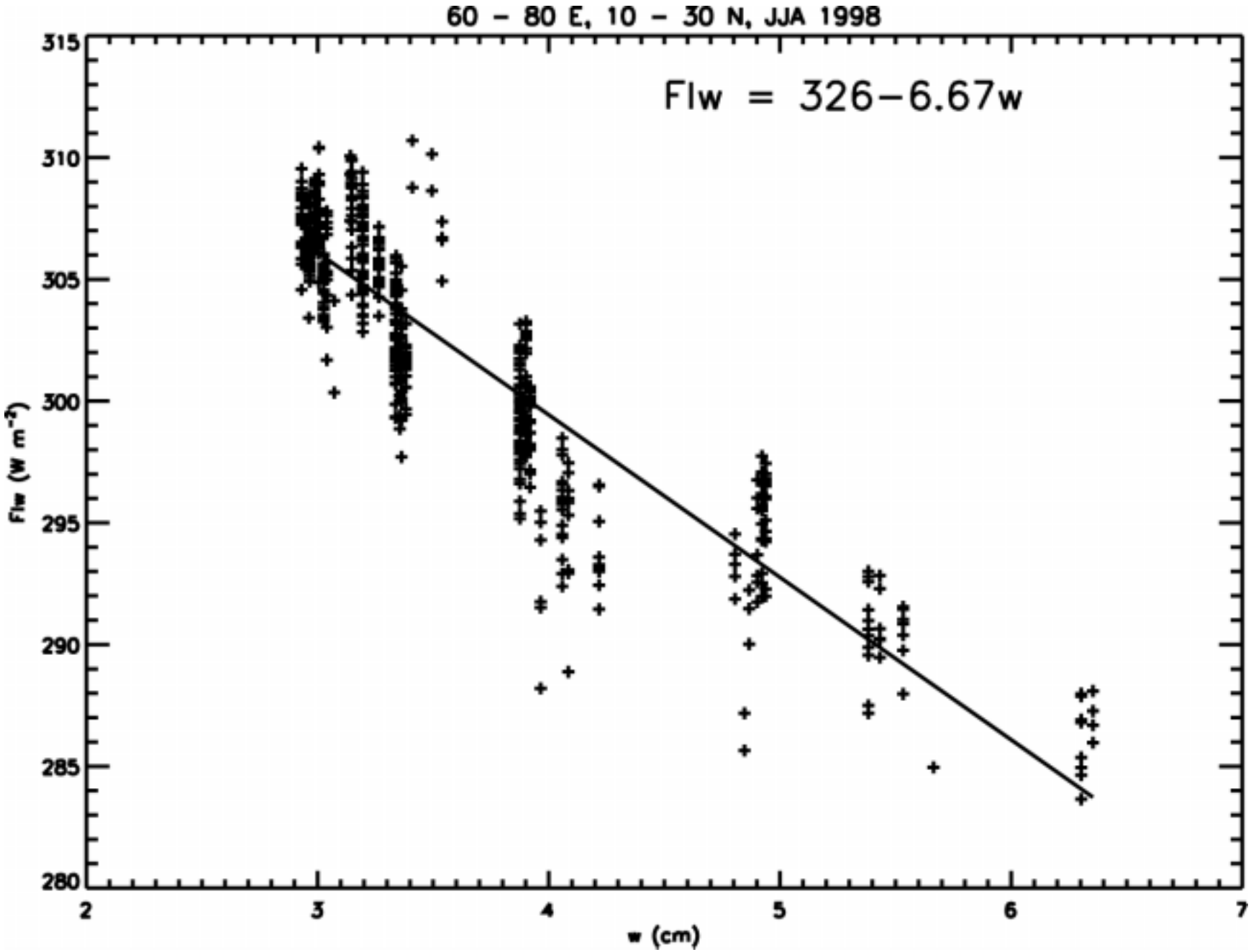
60 – 80 E, 10 – 30 N, JJA 1998
FIw = 326−6.67w
FIw (W m⁻²)
w (cm)
315
310
305
300
295
290
285
280
2
3
4
5
6
7

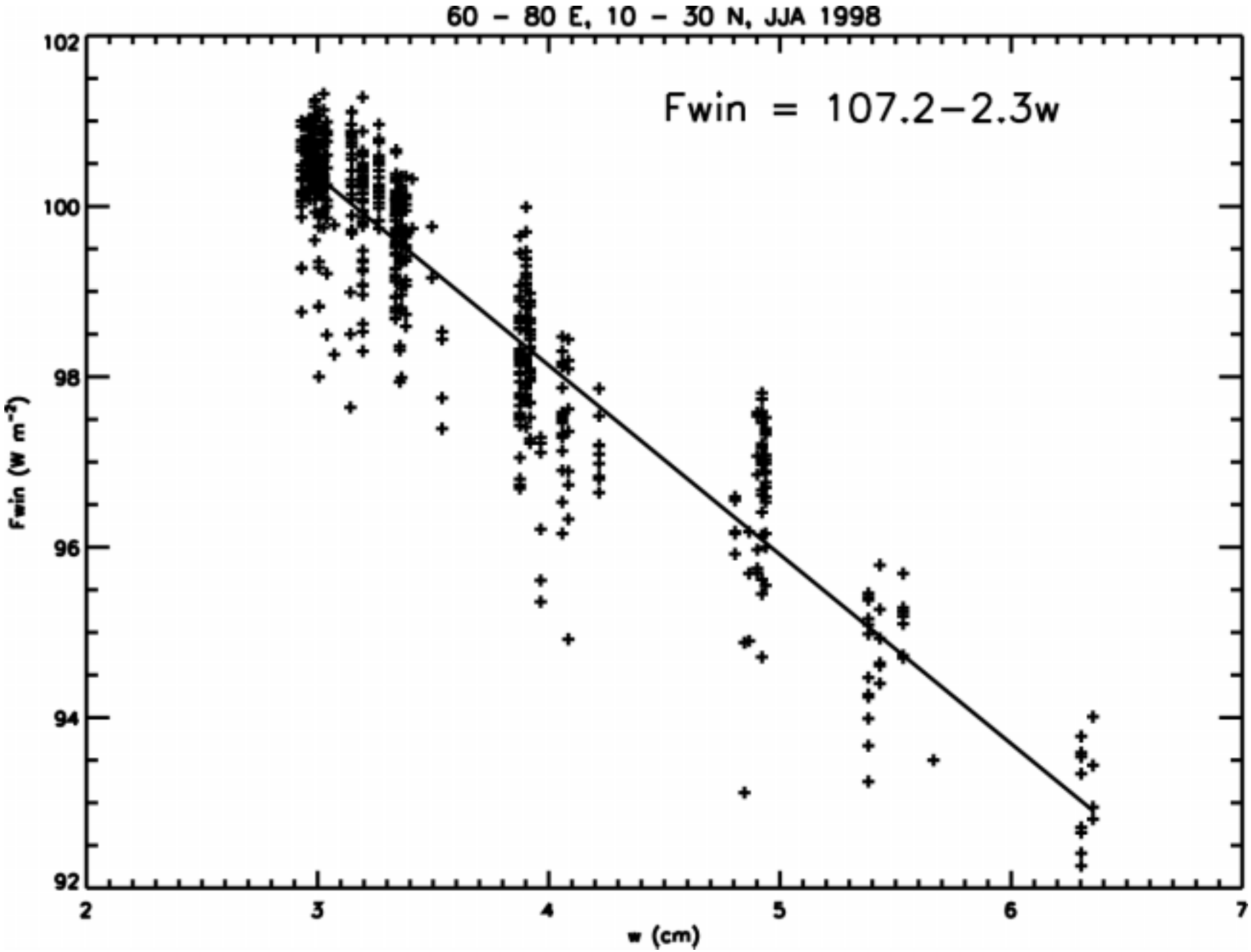
60 – 80 E, 10 – 30 N, JJA 1998
Fwin = 107.2−2.3w
Fwin (W m⁻²)
w (cm)
102
100
98
96
94
92
2
3
4
5
6
7

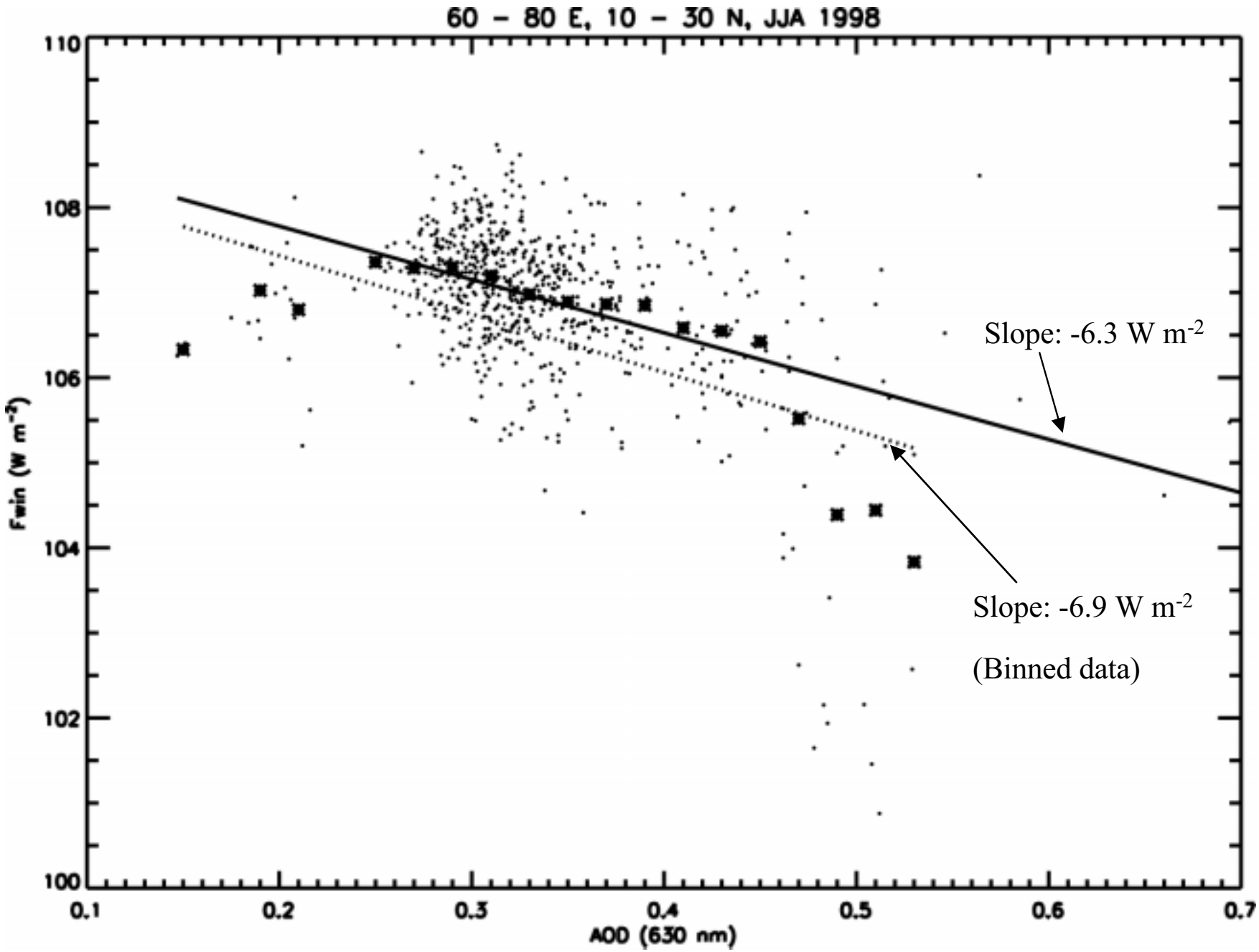
60 – 80 E, 10 – 30 N, JJA 1998
Fwin (W m-2)
AOD (630 nm)
110
108
106
104
102
100
0.1
0.2
0.3
0.4
0.5
0.6
0.7
Slope: -6.3 W m-2
Slope: -6.9 W m-2
(Binned data)

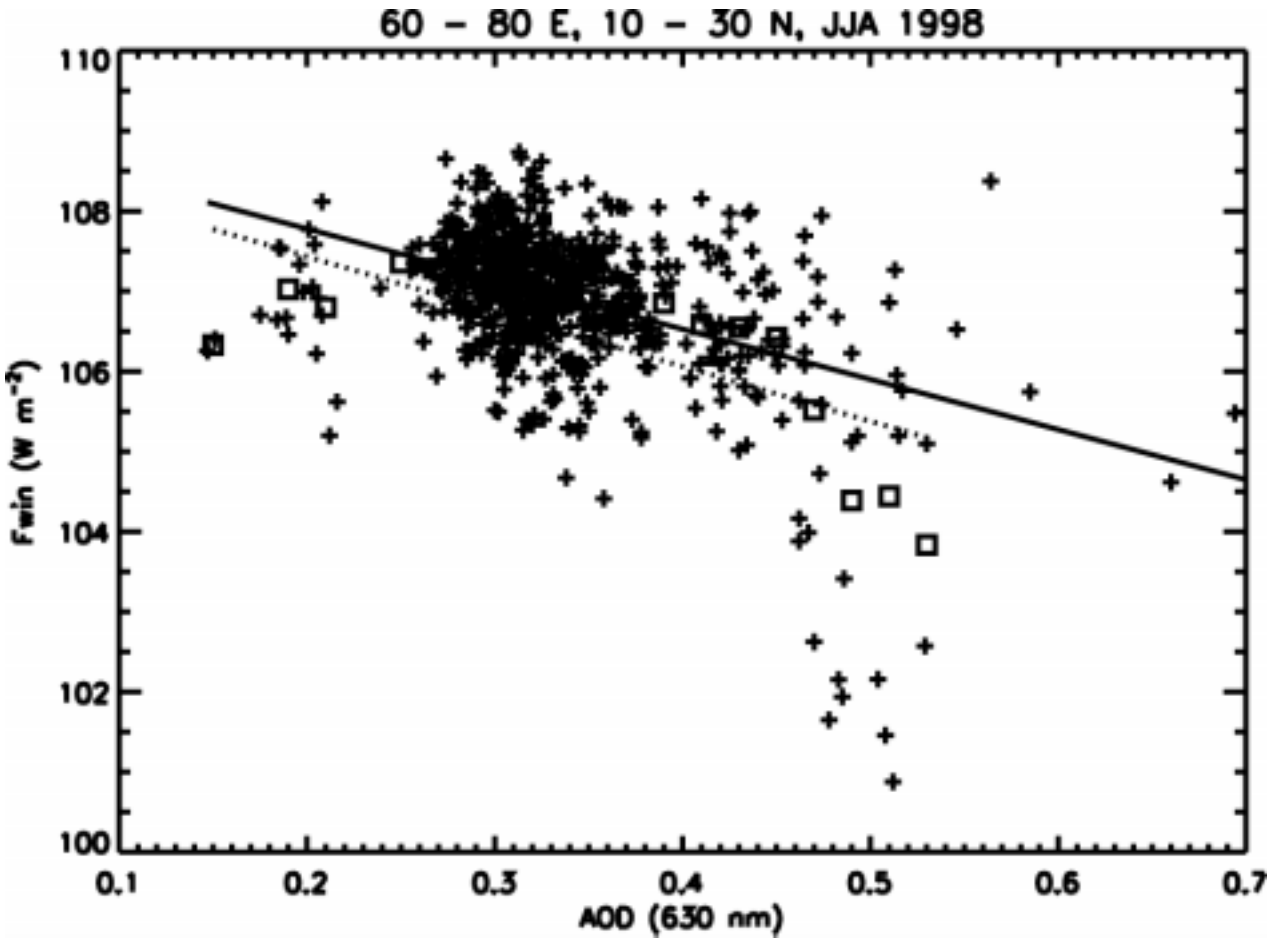
60 – 80 E, 10 – 30 N, JJA 1998
110
108
106
104
102
100
Fwin (W m⁻²)
0.1
0.2
0.3
0.4
0.5
0.6
0.7
AOD (630 nm)

Comparison with other studies

- Hsu, Herman & Weaver (2000 JGR) using TOMS & ERBE obtain forcing efficiency of –21 to 24 W m^{-2} for the same region for July 1985.